Journal of Materials Chemistry A

Multipurpose [1,2,4]Triazolo[4,3-b][1,2,4,5] Tetrazine-based Energetic Materials

Journal:	*Journal of Materials Chemistry A*
Manuscript ID	TA-ART-02-2019-001717.R2
Article Type:	Paper
Date Submitted by the Author:	08-Mar-2019
Complete List of Authors:	Shreeve, Jean'ne; University of Idaho, Department of Chemistry Liu, Yingle; Sichuan University of Science and Engineering, Zhao, Gang; University of Idaho, Chemistry Tang, Yongxing; University of Idaho, Chemistry Zhang, Jichuan; University of Idaho, Chemistry Hu, Lu; University of Idaho, Chemistry Imler, Gregory; US Naval Research Laboratory, Crystallography Parrish, Damon; Naval Research Laboratory,

Journal Name

ARTICLE

Multipurpose [1,2,4]Triazolo[4,3-b][1,2,4,5] Tetrazine-based Energetic Materials

Received 00th January 20xx,

Accepted 00th January 20xx

DOI: 10.1039/x0xx00000x

www.rsc.org/

Yingle Liu,* [a,b] Gang Zhao, [b] Yongxing Tang,[b] Jichuan Zhang,[b] Lu Hu,[b] Gregory H. Imler,[c] Damon A. Parrish,[c] Jean'ne M. Shreeve*[b]

Two series of [1,2,4]triazolo[4,3-b][1,2,4,5]tetrazine-based energetic materials were synthesized effectively by using monosubstituted tetrazine or terazine-based fused rings as starting materials. Among them, compound **5** exhibits excellent insensitivity toward external stimuli (IS = 43 J and FS > 360 N) and a very good calculated detonation performance (Dv = 9408 m s^{-1} and P = 37.8 GPa) that are comparable to the current secondary-explosive benchmark, CL-20, which strongly suggests **5** as a secondary explosive. The azo compound **10** has a remarkable measured density of 1.91 g cm^{-3} at 20 ℃, excellent thermal stability (T_d = 305 ℃), and very good calculated detonation performance (Dv = 9200 m s^{-1} and P = 34.8 GPa), which outperforms all current heat-resistant explosives. Compound **10** has a significant potential as a heat-resistant explosive. Compounds **14**, **17** and **19** are very sensitive (IS ⩽ 2 J and FS ⩽100 J) but exhibit excellent calculated detonation performance (Dv ⩾ 9236 m s^{-1} and P ⩾ 36.3 GPa) which are very high values among current azide-containing primary explosives. These attractive features suggest strong possibilities for applications as primary explosives. A detailed study based on X-ray diffraction is used to illustrate the relationship between weak interactions and sensitivity of energetic materials. Attempts were made to design next-generation fused ring energetic materials for different applications as an alternating kind or site of the substituent group(s).

Introduction

As a fascinating class of high-energy density materials (HEDMs), nitrogen-rich energetic materials are an intensively investigated area of material science which can be used as propellants, explosives and pyrotechnics to satisfy the growing demand for military and civilian uses.[1]Through the developing history of energetic materials, it is seen that the methodology for designing energetic materials has changed markedly. The goal for traditional development of energetic materials addressed adjusting the proportion of different explosive ingredients as a means to enhance detonation performance.[2] However, in order to meet the growing environmental and safety requirements, modern energetic materials are not only required to be high energy but also environmentally friendly, thermally stable, highly dense, and nitrogen- and oxygen-rich.[3] As a result, fused nitrogen-rich heterocycle frameworks with conjugated systems are of particular interest in the development of modern energetic materials due to the high thermal stabilities and low sensitivities toward destructive stimuli.[4] Additionally, the high nitrogen content of fused rings normally indicates a higher heat of formation than an ordinary single ring with concomitant tremendous energy release.[5] As a result of these advantages, some milestone fused ring systems have been synthesized in recent years and have shown excellent performance.[6]

Based on the proposed applications, energetic materials can be divided generally into several subclasses, including secondary, primary, and heat-resistant explosives, as well as fuel-rich solid propellants, and propellant oxidizers.[7] Classification as a secondary explosive requires energetic materials possessing excellent detonation properties and low sensitivity to external stimuli.[8] However, just a few instances exist where excellent energetic performance and insensitivity occur because these parameters are often contradictory.[9] Recently, two groundbreaking energetic salts **I** and **II** (Figure 1), which are derivatives of fused rings, and which possess very good insensitivities and excellent detonation velocities that are higher than the values of the commonly used secondary explosives, TATB and LLM-105, were synthesized.[10] A primary explosive is a class of energetic materials with excellent detonation performance and sensitivity used to initiate a larger mass of secondary explosives.[11] In the last several decades, lead-based primary explosives, such as lead azide (LA) and lead styphnate (LS), were used widely due to their superior initiating and priming abilities compared with other copper- or potassium-based primary explosives.[12] However, lead contamination from the use of lead-

[a] School of Chemistry and Environmental Engineering, Sichuan University of Science & Engineering, 180 Xueyuan Street, Huixing Lu, Zigong, Sichuan 643000 (China). E-mail: liuyingleyou@163.com
[b] Department of Chemistry, University of Idaho, Moscow, ID 83844-2343, USA. E-mail: jshreeve@uidaho.edu
[c] Naval Research Laboratory, Code 6910, 4555 Overlook Ave., Washington, DC 20375 USA.

† Electronic Supplementary Information (ESI) available: CCDC 1884779; 1884780; 1884783-1884785. For ESI and crystallographic data in CIF or other electronic format see DOI: 10.1039/x0xx00000x

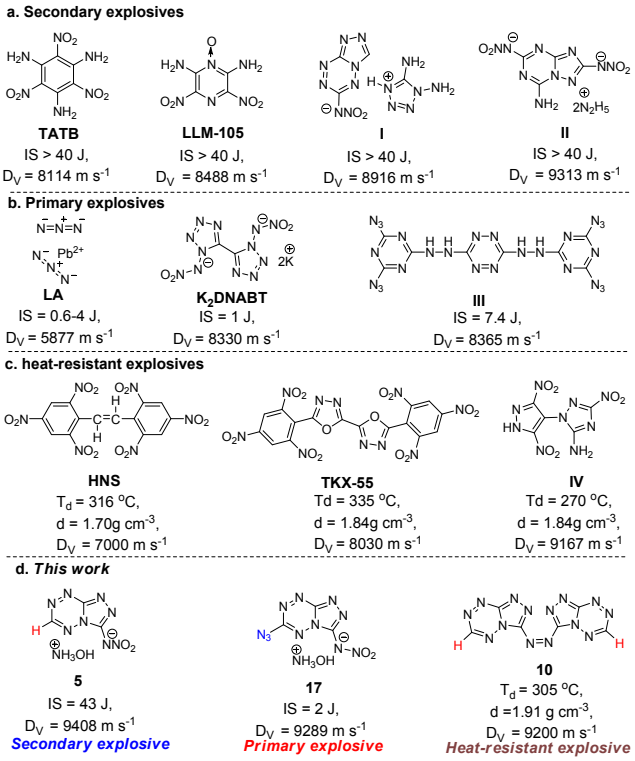

Fig. 1 Different applications for energetic materials in previous studies and this study.

based primary explosives has played a huge threat to personal health and environment.[13] In 2018, a metal-free environmentally friendly primary explosive, **III,** with a good calculated detonation velocity (D_V = 8365 m s^{-1}) that is better than the value for LA (D_V = 5877 m s^{-1}) was developed. Additionally, several initiation ability tests show that azido compound, **III**, generates an intense shockwave to initiate a larger mass of RDX, thus paving the road to develop metal free, azido-containing high-performance primary explosives.[14] Heat-resistant explosives are a type of explosive with high thermal stability (T_d ≥ 250 °C), low vapor pressure and high detonation performance which can be used in oil-well drilling, space exploration, and safer explosive production.[15] The original thermal resistant explosives were polynitrobenzene compounds with high decomposition temperatures (>300 °C) and low detonation velocity (D_V < 8300 m s^{-1}).[16] In 2016, the first azole-based thermal resistant explosive, **IV**, that showed an acceptable decomposition temperature (T_d = 270 °C) and excellent detonation velocity (D_V = 9167 m s^{-1}) was reported.[17]

Considering that different substituents have important effects on the mechanical sensitivity of energetic materials,[18] achieving a secondary explosive with both excellent energetic performance and insensitivity is a challenge, azido/polyazido-based fused rings as primary explosives and heat-resistant explosives are yet to be investigated. Now we report the synthesis of N-([1,2,4]triazolo[4,3-b][1,2,4,5]tetrazin-3-yl)nitramide (**3**), 1,2-bis([1,2,4]triazolo [4,3-b][1,2,4,5] tetrazin-3-yl)diazene (**10**), N-(6-azido-[1,2,4]triazolo[4,3-b] [1,2,4,5]tetrazin-3-yl) nitramide (**14**), 1,2-bis(6-azido-[1,2,4]triazolo[4,3-b][1,2,4,5]tetrazin-3-yl) diazene (**19**), and their salts. Each exhibits very different mechanical sensitivity, which highlights their application potential as secondary, metal-free primary or heat-resistant explosives, respectively. A detailed study based on X-ray diffraction has been used to illustrate the relationship between weak interactions (π-π interactions,[19] hydrogen-bonds,[10b] between azido groups) and the mechanical sensitivity of energetic materials. We hoped to design next-generation fused ring energetic materials for different applications by regulating mechanical sensitivity using this alternating kind or site of functional group strategy.

Results and discussion

Synthesis

The synthetic pathway to monosubstituted energetic materials, **3-10,** is given in Scheme 1. 3-Monosubstituted 1,2,4,5-tetrazine, **1**, synthesized according to the literature,[20] was treated with cyanogen bromide in aqueous 0.5 M HCl solution to obtain [1,2,4]triazolo[4,3-b][1,2, 4, 5] tetrazine, **2**. Nitration of **2** was carried out by using 100% nitric acid to give the nitramino compound **3** as an orange solid. When **3** was reacted with aqueous ammonia, hydroxylamine or guanidine carbonate, three salts, **4-6**, were obtained in high yields. However, the reaction of **3** with hydrazine hydrate led to an unidentified black mixture. Fortunately, the pure hydrazinium **8** or triaminoguanidinium **9** salts were obtained by metathesis reactions of silver salt **7** with hydrazine hydrochloride or triaminoguanidine hydrochloride, respectively. Since the azo linkage is an efficient way to connect two energetic components, we attempted to prepare azo compound **10** by using a

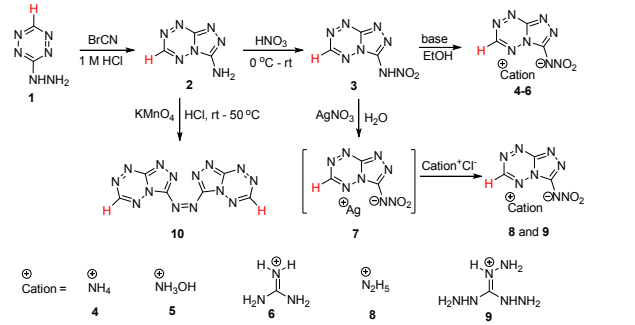

Scheme 1 Preparation of energetic monosubstituted fused ring materials **4-6** and **8-10**

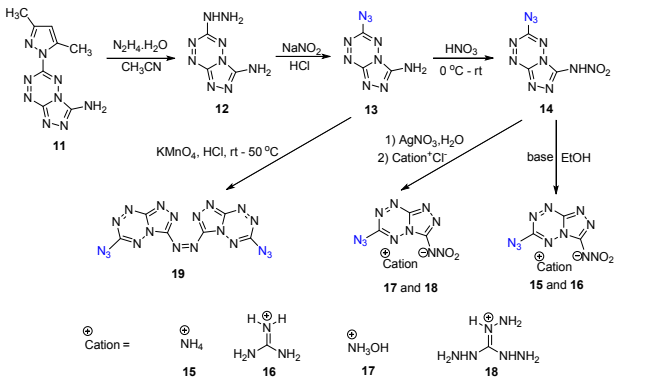

Scheme 2 Preparation of monosubstituted fused ring energetic materials **13-19**

variety of oxidants. Acidic potassium permanganate solution was found to be a useful reactant to give yellow solid **10** in good yield.

Azido-containing energetic compounds **13**-**19** were synthesized (Scheme 2). The fused heterocycle **12** was produced by nucleophilic substitution of compound **11**[21] with hydrazine hydrate. 6-Azido-[1,2,4]triazolo[4,3-b][1,2,4,5]tetrazin-3-amine **13** was obtained from the diazotization reaction of **12** with $NaNO_2$. Then, the neutral nitroamine compound, **14**, the energetic salts, **15**-**18**, and diazido containing azo compound, **19**, were synthesized successfully using the route given in Scheme 2.

Spectral and single crystal X-ray diffraction studies of compounds

All of the new compounds were fully characterized by multinuclear NMR spectroscopy and IR spectral analysis as well as elemental analysis. Single-crystals suitable for X-ray diffraction studies were obtained by slow evaporation of a solution of ethyl alcohol and a few drops of water (**3**, **5**, **14** and **17**) or DMSO (**13**). Crystal structures of these compounds are given in Figure 2. Because of the presence of the conjugated fused rings, the structures of the neutral compounds or their anions are all nearly planar.

N-([1,2,4]triazolo[4,3-b][1,2,4,5]tetrazin-3-yl)nitramide (**3**) crystallizes in the orthorhombic space group, $Pna2_1$, with eight molecules in each lattice cell (Z = 8). The density of **3** is 1.814 g cm^{-3} at 20 °C, which is higher than its isomer N-([1,2,4]triazolo[4,3-b][1,2,4,5]tetrazin-6-yl)nitramide (**3-isomer**)[10b] (1.740 g cm^{-3} at 20 °C) that has good stability toward mechanical stimulus. Crystal and charge distribution data calculated using natural bond orbital (NBO) charge analysis[22] for compounds, **3** and **3-isomer** gave the results shown in Figure 3. The lengths of C-N, N-N, or N=N bonds in the ring of **3** are in the range of 1.276 1.398 Å which are slightly shorter than those found in the **3-isomer** (1.281 1.408 Å). The packing coefficient 0.72 for **3** is larger than 0.70 for the **3-isomer**. The range of charge distribution on the atoms of fused ring **3** is -0.240 -0.475, which is slightly narrower than -0.245 -0.496 for the **3-isomer**. These results suggest that **3** should be more aromatic and less sensitive toward external stimuli than its isomer.

The hydroxylammonium salt, **5,** crystallizes as a clear orange block crystal in the monoclinic space group with Cc symmetry and four molecules in each lattice cell (Z = 4). Each hydroxylammonium cation interacts with three other molecules through hydrogen-bonding, cation-anion contact and other weak associations including N···N, N···O and O···O interactions, which assists these three

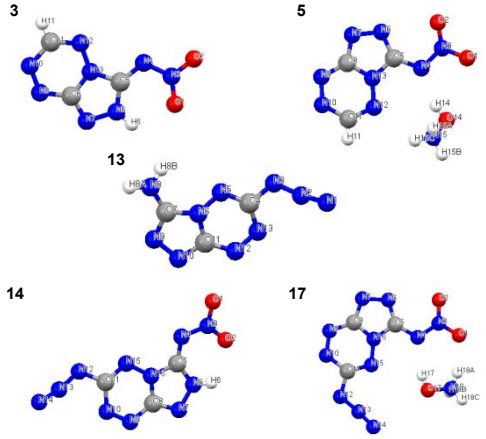

Fig. 2 Single-crystal X-ray structures of **3**, **5**, **13**, **14** and **17**.

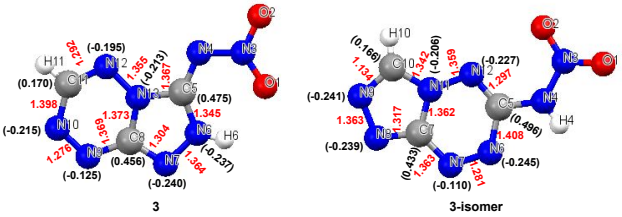

Fig. 3 Length of bonds (red numbers) and charge distribution (in parentheses) of **3** and **3-isomer**

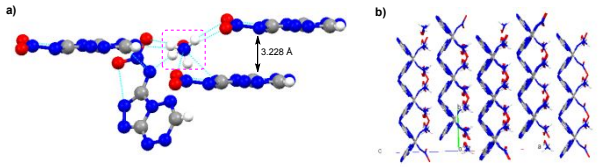

Fig. 4 (a) The intermolecular weak interactions of **5**. (b) The packing diagram of **5**.

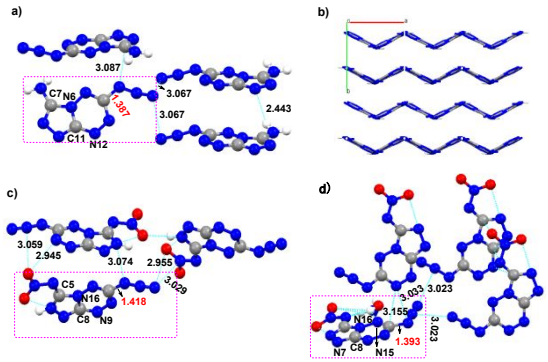

Fig. 5 (a) The intermolecular interactions of **13**. (b) The packing diagram of **13**. (c) The intermolecular interactions of **14**. (d) The intermolecular interactions of **17**.

molecules in creating a parallel stacking arrangement (interlayer distance = 3.228 Å) (Figure 4). As a result, the packing coefficient of **5** is 0.76 and its density is 1.832 g cm^{-3} at 20 °C.

6-Azido-[1,2,4]triazolo[4,3-b][1,2,4,5]tetrazin-3-amine, **13,** crystallizes in the orthorhombic space group, with a density of 1.763 g cm^{-3} at 20 °C. In addition to hydrogen bonds, there are C-N and N-N interactions between the azido group of one molecule and three other molecules in the range of 3.067 3.087 Å (Figure 5a). These three molecules are essentially parallel. Because of this kind of weak directional interaction, **13** is found in a wave-like stacking arrangement with a packing coefficient of 0.72(3) (Figure 5b). Compounds **14** and **17** are in the monoclinic space group with $P2_1$ symmetry with crystal densities of 1.853 g cm^{-3} and 1.787g cm^{-3}, respectively. Due to the presence of the nitroamine group and the modification of the salts, the bond length between the azide moiety and fused ring increases from 1.387 Å for **13** to 1.418 for **14**, to 1.393 for **17**, and the coplanarity of the fused rings is also decreased because the dihedral angle C(7)-N(6)-C(11)-N(12) of **13** is 177.36° which has changed to N(9)-C(8)-N(10)-C(5) = 177.01° for **14** and N(15)-N(16)-C(8)-N(7) = 175.13° for **17**. Furthermore, the azido group of **14** or **17** interacts with other two or three molecules in the crystal and these molecules are irregularly distributed in three dimensions. Based on these reasons, **14** and **17** showed low packing coefficients of 0.72(5) and 0.72(6), respectively.

Table 1 Energetic properties of compounds **3-6, 8-10** and **13-19.**

Comp.	N%	T_{dec}[a] (°C)	P[b] (g cm^{-3})	ΔH_f[c] (kJ mol^{-1}/kJ g^{-1})	Dv[d] (m s^{-1})	P[e] (GPa)	IS[f] (J)	FS[g] (N)
3	61.5	132	1.81	647.8/3.56	8880	33.2	31	>240
4	63.3	193	1.79	705.0/3.54	9129	33.4	33	>360
5	58.6	150	1.83	751.2/3.49	9408	37.8	43	>360
6	63.9	280	1.79	678.6/2.81	8932	30.7	50	>360
8	65.4	123	1.79	858.4/4.01	9416	35.7	32	>360
9	68.5	156	1.78	1009.7/3.10	8486	28.0	8	>240
10	71.1	305	1.91	1525.2/5.64	9200	34.8	16	>360
13	78.6	165	1.74	913.6/5.13	8581	28.5	30	>45
14	69.1	150	1.85	951.8/4.27	9236	36.3	1	>40
15	70.0	180	1.77	1055.6/4.40	9149	34.3	1	>160
16	69.2	170	1.76	1026.0/3.64	8879	31.0	13	>160
17	65.6	156	1.79	1106.3/4.32	9289	36.8	2	>100
18	72.8	129	1.74	1352.6/4.13	9180	32.7	1	>40
19	79.5	183	1.77	2194.6/6.23	8690	30.2	1	<5
RDX	37.8	204	1.80	70.3/0.36	8795	34.9	7.4	120
HMX	37.8	280	1.90	105.0/0.25	9320	39.5	7	120
CL-20	38.4	210	2.03	397.8/0.90	9406	44.6	4	94
HNS	18.7	318	1.74	78.2/0.17	7612	24.3	5	240
IV	44.2	270	1.84	833.4/2.92	9167	37.8	9	240
$Pb(N_3)_2$	28.9	315	4.80	450.1/1.55	5855	33.4	0.6-4	0.3-0.5
III	78.4	194	1.76	2113.6/4.55	8365	26.8	7.4	35.3

[a] Decomposition temperature (onset). [b] Density measured by a gas pycnometer at 25 °C. [c] Calculated molar enthalpy of formation in solid state. [d] Calculated detonation velocity. [e] Calculated detonation pressure. [f] Impact sensitivity. [g] Friction sensitivity.

Physicochemical and energetic properties

The thermal behavior of all energetic compounds was determined by differential scanning calorimetric (DSC) measurements at a heating rate of 5 °C min^{-1} (Table 1). Most compounds (**3**-**6**, **8**-**10**, and **13**-**19**) decompose without melting. Among them, azo compound **10** exhibits the best thermal stability with an onset decomposition temperature at 305 °C, but the azo compound **19** decomposes at 183 °C. This can be explained by the higher bond-dissociation energy (BDE) for **10** at 265.38 kJ mol^{-1} while at 99.65 kJ mol^{-1} for **19** (Fig. S21). Other compounds have thermal decomposition temperatures between 123 °C and 280 °C.

The experimental densities of all fused rings compounds were obtained by using a gas pycnometer (25 °C) and found to range between 1.74 and 1.91 g cm^{-3}. These are comparable to the currently used typical HEDMs, such as RDX (1.80 g cm^{-3}) and HMX (1.91 g cm^{-3}). Among them, the hydroxylammonium salt, **5,** is more dense (1.83 g cm^{-3}) than the parent neutral fused ring **3** (1.81 g cm^{-3}) which is monosubstituted with a nitroamino group. However, the density of hydroxylammonium salt, **17** (1.79 g cm^{-3}) is considerably lower than its parent fused ring **14** (1.85 g cm^{-3}**)** substituted by azido and nitroamino group. From this fact, it is obvious that the introduction of substituents has a great influence on the spatial arrangement of molecules and density. It is noteworthy that **10** as a CHN azo energetic material has a higher crystal density of 1.911g cm^{-3} than some reported single ring-based CHN azo derivatives, for example, 1,2-di(1H-tetrazol-1-yl)diazene[22] (1.774 g cm^{-3} at 25 °C) and 6,6'-(diazene-1,2-diyl)bis(1,2,4,5-tetrazin-3-amine) (1.84 g cm^{-3} at 25 °C).[23] The remarkably higher density of **10** may be attributed to larger conjugated system and face-to-face π-π interactions. The Heats of formation, were calculated using the Gaussian03 (Revision D. 0.1) suite of programs based on isodesmic reactions (Scheme S1) or the Born-Haber cycle.[24] Due to the presence of a large number of N–N or C–N bonds in the fused rings, these two series of compounds possess comparable high nitrogen content, such as **10** (71.1%), **13** (78.6%), **15** (70.0%), **18** (72.8%) and **19** (79.5%). As a result, all of the fused rings have relatively high positive heats of formation ($\geqslant$2.81 kJ g^{-1}) exceeding the value for CL-20 (0.90 kJ g^{-1}) markedly. Among them, the diazido-containing azo compound, **19**, possesses the highest positive heat of formation of 6.23 kJ g^{-1}. This value is larger than 4.56 kJ g^{-1} for **III**[14] and 4.44 kJ g^{-1} for 5-(5-azido-1H-1,2,4-triazol-3-yl)tetrazole[25] which are two of the most recently reported binary CHN primary explosives. Furthermore this value is also very close to 6.20 kJ g^{-1} for 1,2-di(1H-tetrazol-1-yl)diazene[22] and 6.71 KJ g^{-1} for 3,6-diazido-1,2,4,5-tetrazine[1b] which has been claimed to have the highest heat of formation for a binary CN compound. Among these reported four compounds, the nitrogen content of the binary CHN primary explosive are 78.4% for **III** and 78.6% for 5-(5-azido-1H-1,2,4-triazol-3-yl)tetrazole, which approach the 79.5% of compound **19**. Based on these facts, we show that the formation of fused rings have a positive effect on the heat of formation of compounds.

With the measured densities and calculated heats of formation in hand, detonation performance of these energetic compounds were calculated by using EXPLO5 (v 6.01).[26] As shown in Table 1, the calculated detonation velocities are found in the range 8486 to 9416 m s^{-1}. The values of **5** (9408 m s^{-1}) and **6** (9416 m s^{-1}) are comparable to CL-20 (9406 m s^{-1}), The detonation pressures fall between 28.0 and 37.8 GPa with values in some cases exceeding

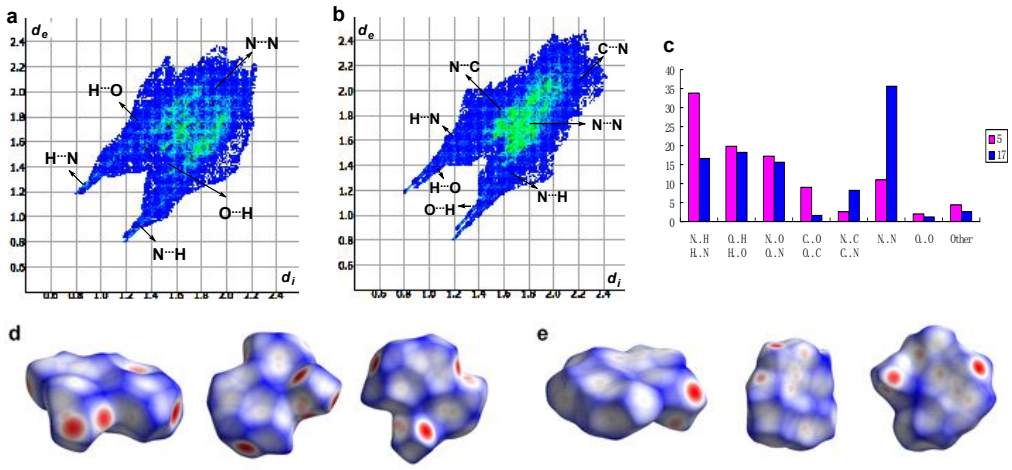

Fig. 6 2D fingerprint plots in crystal stacking for (a) **5** and (b) **17**. In image c, the individual atomic contacts percentage in the bar graphs for **5** and **17**. Images d and e show the Hirshfeld surfaces for **5** and **17** molecules (white, distance d = the van der Waals distance; blue, d > the van der Waals distance; red, d < van der Waals distance).

RDX (34.9 GPa) and being close to HMX (39.5 GPa). Among them, the calculated detonation performance for **19** (D_V = 8690 m s^{-1}, P = 30.2 GPa) is better than the values of **III**[14] (D_V = 8365 m s^{-1}, P = 26.8 GPa) and 5-(5-azido-1H-1,2,4-triazol-3-yl)tetrazole[25] (D_V = 7874 m s^{-1}, P = 24.1 GPa) which are two recently reported primary explosives.

In addition to excellent detonation performance, the requirement of sensitivity to external stimuli for energetic materials with different application purposes varies greatly. Secondary explosives tend to have good insensitivity (IS > 40J, FS > 360 N), while primary explosives require compounds with higher sensitivity (IS ≤ 3 J, FS < 80 N). Impact (IS) and friction (FS) sensitivity measurements of these fused rings compounds were obtained by using standard BAM drop hammer and friction tester technology, respectively.[27] In the series of monosubstituted fused ring compounds (**3**-**6** and **8**-**10**), not surprisingly the neutral **3** shows lower sensitivity (IS = 31 J, FS > 240 N) than its isomer (IS = 20 J, FS > 240 N).[10b] By pairing with small volume nitrogen-rich cations, the energetic salts of **3** (**4**-**6** and **8**) exhibit low impact and friction insensitivity (IS, 32-50 J; FS > 360 N) because of the negative charge delocalization on the nitroamine moieties, and hydrogen bonding with the anions. But neutralization with triaminoguanidine, a large volume nitrogen-rich base, gives rise to the corresponding salt **9** which is highly sensitive (IS = 8 J, FS > 240N). This is likely the result of a poor crystal stacking pattern. The azo compound **10** is moderately sensitive (IS = 16 J, FS > 360 N) to external stimuli, which mainly arises from the short interlayer distance for the crystal packing which could be extrapolated from the high density. In the series of disubstituted fused ring compounds (**13**-**19**), all but **13** (IS = 30 J, FS > 45 N) and **16** (IS = 13J, FS > 160N) are extremely sensitive (IS, 1-2 J; FS, 5-160 N) because of the irregularity of the three dimensional crystal stacking. It should be noted that compound **19** (IS = 1 J, FS < 5 N) is the most sensitive.

To gain further information about sensitivity differences between these two series of compounds, weak interactions in representative compounds **5** and **17** were investigated via Hirschfeld surfaces and 2D fingerprint plots.[28] As shown in Figures 6 d and e, the surfaces of these two compounds have plate shapes because of coplanar conjugated molecular structures. Furthermore, some red dots mainly caused by the intermolecular H···O, O···H, H···N and N···H interactions were found on the edges of each plate-like surface. The populations of these weak interactions can also be directly achieved by the 2D fingerprint plots. From Figure 6 a and c, the hydrogen bonding possesses 53.6% of the total weak interactions for **5** (Fig. S21). Considering the fact that hydrogen bonding as a "soft" interaction has a stabilizing action toward impact and friction sensitivities has been comfirmed by previous studies,[10b,18 and 29] so it is readily understood that **5** (IS = 43 J; FS > 360N) is very insensitive. However, the sum of proportions of N···N, N···C and C···N for **17** is 43.9% which mainly comes from the interaction of azide groups irregularly distributed in three-dimensional space (Fig. S22). Mechanical stimuli from any orientation easily cause molecular decomposition because of the "hard" linear azide functional groups completely suspended on the outside of the fused ring. Thus, it is not surprising that this compound is very sensitive (IS = 2J; FS > 100N).

Conclusion

In conclusion, two series of [1,2,4]triazolo[4,3-b][1,2,4,5]tetrazine-based energetic materials were effectively synthesized by using versatile energetic unit strategies. All the new compounds were fully characterized with IR, multinuclear NMR, and elemental analysis and five compounds were further confirmed by X-ray diffraction. Because of the large conjugated system and nearly planar structure, these compounds derived from monosubstituted fused rings possess excellent low sensitivity properties. Compound **5** which is similar to TATB is especially insensitive to mechanical stimuli and its calculated detonation velocities and pressures are comparable to the current secondary-explosive benchmark **CL-20**, thus highlighting its application potential as a secondary explosive. The azo compound **10** was found to possess a high density, excellent thermal stability, and excellent detonation performance. It outperforms all currently used heat-resistant explosives, for example, HNS, PYX, TKX-55, and IV. Therefore, compound **10** has a significant application potential as a heat-resistant explosive. Compounds **14**, **17**, and **19** have extremely high sensitivities

because of the interaction between different azide groups which are suspended on the outside of the fused ring in three-dimensional space. These materials exhibit excellent calculated detonation performances whose values are extremely high among current azido primary explosive, such as **III.** They exhibit good possibilities for application as primary explosives.

Experimental section

Caution!

Although no explosions were observed during the syntheses and handing of these compounds in this study, all manipulations should be carried out in a hood and behind a safety shield. Mechanical actions involving scratching or scraping must be avoided. Eye protection and leather gloves should be worn. All of the energetic compounds must be synthesized on a small scale.

General methods

All reagents were purchased from AKSci, VWR or Alfa Aesar in analytical grade and were used as supplied. ^{1}H and ^{13}C NMR spectra were recorded on a Bruker 300 MHz NMR spectrometer or 500 MHz (Bruker AVANCE 500) nuclear magnetic resonance spectrometer. Chemical shifts for ^{1}H, and ^{13}C NMR spectra are reported relative to $(CH_3)_4Si$. $[D_6]$DMSO was used as a locking solvent unless otherwise stated. Infrared (IR) spectra were recorded on an FT-IR spectrometer (Thermo Nicolet AVATAR 370) as thin films using KBr plates. Density was determined at room temperature by employing a Micromeritics AccuPyc II 1340 gas pycnometer. Melting and decomposition (onset) points were recorded on a differential scanning calorimeter (DSC, TA Instruments Q2000) at a scan rate of 5 °C min^{-1}. Elemental analyses (C, H, N) were performed on a Vario Micro cube Elementar Analyser. Impact and friction sensitivity measurements were made using a standard BAM Fall hammer and a BAM friction tester.

Computational methods

The gas phase enthalpies of formation were calculated based on isodesmic reactions (Scheme S1, ESI†). The enthalpy of reaction is obtained by combining the MP2/6-311++G** energy difference for the reactions, the scaled zero point energies (ZPE), values of thermal correction (HT), and other thermal factors. The solid state heat of formation of **3, 10, 13, 14 and 19** were calculated with Trouton's rule according to eqn (1) (T represents either the melting point or the decomposition temperature when no melting occurs prior to decomposition).[30]

$$\triangle H_{sub} = 188/\text{J mol}^{-1}\,\text{K}^{-1} \times T \quad (1)$$

For other energetic salts, the solid-phase enthalpy of formation is obtained using a Born–Haber energy cycle.[31]

X-ray crystallography data

A clear orange chunk crystal (**3**) of dimensions 0.316 x 0.117 x 0.075 mm^{-3}, a clear orange block crystal (**5**) of dimensions 0.121 x 0.108 x 0.040 mm^{-3}, a clear orange plate crystal (**13**) of dimensions 0.219 x 0.195 x 0.020 mm, a clear orange block crystal (**14**) of dimensions 0.275 x 0.140 x 0.052 mm, or a clear orange needle crystal (**17**) of dimensions 0.592 x 0.076 x 0.030 mm was mounted on a MiteGen MicroMesh using a small amount of Cargille immersion oil. Data were collected on a Bruker three-circle platform diffractometer equipped with a SMART APEX II CCD detector. All of crystals were irradiated using graphite monochromated MoK_α radiation (λ= 0.71073) and all of data were collected at room temperature (20 °C).

Data collection was performed and the unit cell was initially refined using *APEX3* [v2015.5-2].[32] Data reduction was performed using *SAINT* [v8.34A][33] and *XPREP* [v2014/2].[34] Corrections were applied for Lorentz, polarization, and absorption effects using *SADABS* [v2014/2].[35] The structure was solved and refined with the aid of the program SHELXL-2014/7.[36] The full-matrix least-squares refinement on F^2 included atomic coordinates and anisotropic thermal parameters for all non-H atoms. Hydrogen atoms were located from the difference electron-density maps and added using a riding model.

5-Cyano-N'-hydroxy-2-methyl-2H-1,2,3-triazole-4 carboximidamide (2). Compound **1** [**(**2.26 g 20 mmol)] was dissolved in ethanol (30 mL) and added over 20 min to 50% hydroxylamine solution [1.58 g (24 mmol)]. The solvent was removed under reduced pressure over 2 h. Upon filtering, **2** [3.32 g (94%)] was obtained as a yellow solid. T_m: 127 °C. $T_{d(onset)}$: 183 °C; ^{1}H NMR (d_6-DMSO) δ 10.30 (s, 1H), 5.91 (s, 2H), 4.27(s, 3H) ppm. ^{13}C NMR (d_6-DMSO) δ 144.9, 142.9, 116.7, 111.9, 42.9 ppm. IR (KBr): ῦ 3458, 3351, 2254, 1661, 1600, 1414, 1376, 1611, 941, 829, 737, 703 cm^{-1}; Elemental analysis (%) for $C_5H_6N_6O$ (166.06): Calcd C 36.15, H 3.64, N 50.58%. Found: C 36.12, H 3.61, N 50.45%.

[1,2,4]triazolo[4,3-b][1,2,4,5]tetrazin-3-amine (2).

To 0.5N HCl (27 mL) was added **1** (1.03 g, 9.2 mmol). BrCN (0.98 g, 9.2 mmol) was then added and the solution was stirred 24 h. The purple precipitate was filter, washed with water and dried to give a red compound **2** in 71% yield. Td 278 °C; ^{1}H NMR (300 MHz, [D6]DMSO) δ 9.46 (s, 1H), 7.51 (s, 2H) ppm; ^{13}C NMR (75 MHz, [D6]DMSO) δ 15..60, 150.55, 147.37 ppm; IR (KBr pellet): ῦ 3083, 2994, 2717, 1834, 1651, 1519, 1374, 1238, 1161, 1051, 1002, 942, 752, 579 cm^{-1}; elemental analysis (%) for $C_3H_3N_7$ (137.0): calcd C 26.28, H 2.21, N 71.51. Found: C 26.35, H 2.27, N 70.78.

N-([1,2,4]triazolo[4,3-b][1,2,4,5]tetrazin-3-yl)nitramide(3).

Coumpound **2** (0.411 g, 3.0 mmol) was added in portions to a mixture of HNO_3 (100%; 10.5 mL) with stirring and cooling at 0 °C. The mixture was stirred for 4 h at room temperature and afterward the solvent was removed by blowing air. Then CF_3COOH (5 mL) was added to the flask. The precipitate formed was collected by filtration and washed with CF_3COOH to give **3** (0.404 g, 74%) as an orange solid. T_d 152 ℃; ^{1}H NMR (300 MHz, [D6]DMSO) δ 10.59 (s, 1H), 9.99 (s, 1H) ppm; ^{13}C NMR (75 MHz, [D6]DMSO) δ 148.21, 147.67, 146.41ppm; IR (KBr pellet): ῦ 3109, 3068, 3046, 1585, 1536, 1421, 1092, 1017, 938, 761, 679 cm^{-1}; elemental analysis (%) for $C_3H_2N_8O_2$ (182.0): calcd C 19.79, H 1.11, N 61.53. Found: C 19.28, H 1.23, N 60.23.

Ammonium [1,2,4]triazolo[4,3-b][1,2,4,5]tetrazin-3-yl(nitro)amide (4)

To a solution of **1** (182 mg, 1 mmol) in ethanol (5 mL) was added 25% aqueous ammonia (1.2mmol, 168 mg). The reaction was stirred at room temperature for 2h and then the solvent was evaporated in vacuo to obtain the desired red product **4** in 92% yield. T_d 193 °C; ^{1}H NMR (300 MHz, [D6]DMSO) δ 9.64 (s, 1H), 7.10 (s, 4H) ppm; ^{13}C NMR (75 MHz, [D6]DMSO) δ 149.81, 149.71, 146.43ppm; IR (KBr pellet): ῦ 3163, 3115, 3081, 2989, 2414, 2296,

1750, 1677, 1538, 1496, 1205, 1053, 1007, 931, 874, 761 cm^{-1}; elemental analysis (%) for $C_3H_5N_9O_2$ (199.1): calcd C 18.09, H 2.53, N 63.31. Found: C 18.07, H 2.60, N 63.08.

Hydroxylammonium [1,2,4]triazolo[4,3-b][1,2,4,5]tetrazin-3-yl(nitro)amide(5).

To a solution of **1** (182 mg, 1 mmol) in ethanol (5 mL) was added hydroxylamine (50 wt. % in H_2O, 83 mg). The reaction was stirred at room temperature for 2h and then the solvent was evaporated in vacuo to obtain the desired product **5**, red solid, 90% yield. T_d 150 °C; ^1H NMR (300 MHz, [D6]DMSO) δ 10.08 (s, 3H), 9.88 (s, 1H), 9.64 (s, 1H) ppm; ^{13}C NMR (75 MHz, [D6]DMSO) δ 149.78, 149.67, 146.44 ppm; IR (KBr pellet): ṽ 3197, 3101, 2986, 2923, 1308, 2186, 1941, 1851, 1757, 1599, 1426, 1209, 1013, 932, 879, 768 cm^{-1}; elemental analysis (%) for $C_3H_5N_9O_3$ (215.1): calcd C 16.75, H 2.34, N 58.60. Found: C, 16.96; H, 2.44; N, 58.93.

Guanidinium [1,2,4]triazolo[4,3-b][1,2,4,5]tetrazin-3-yl(nitro)amide (6).

To a solution of **1** (182 mg, 1 mmol) in ethanol (5 mL) was added guanidinium carbonate (0.21 g, 1. mmol). The reaction was stirred at room temperature for 2h and then the solvent was evaporated in vacuo to obtain the desired product **6**, red solid, 92% yield. T_d 280 °C; ^1H NMR (300 MHz, [D6]DMSO) δ 9.65 (s, 1H), 6.93 (s, 6H) ppm; ^{13}C NMR (75 MHz, [D6]DMSO) δ 157.89, 149.81, 149.80, 146.48 ppm; IR (KBr pellet): ṽ 3118, 3080, 2993, 2211, 1952, 1686, 1543, 1492, 1201, 1016, 934, 880, 757 cm^{-1}; elemental analysis (%) for $C_4H_7N_{11}O_2$ (241.1): calcd C 19.92; H 2.93; N 63.89. Found: C 19.94; H 3.00; N 63.14.

Hydrazinium [1,2,4]triazolo[4,3-b][1,2,4,5]tetrazin-3-yl(nitro)amide (8).

Silver nitrate (0.34 g, 2 mmol) was dissolved in water (5 mL) and added carefully to a solution of **3** (0.36 g, 2.0 mmol) in water (5 mL). The mixture was stirred for 2 h. After filtration, the product was obtained as a red solid **7** (0.50 g). This solid was added to the methanol solution (10 mL) of hydrazinium hydrochloride (120 mg, 1.74 mmol). After stirring for 2 h at room temperature, silver chloride was removed by filtration and washed with a small amount of methanol. The filtrate was concentrated under reduced pressure and dried in vacuum to yield **8**, red solid, 74% yield. T_d 123 °C; ^1H NMR (300 MHz, [D6]DMSO) δ 9.64 (s, 1H), 7.50 (s, 5H) ppm; ^{13}C NMR (75 MHz, [D6]DMSO) δ 149.80, 149.78, 146.43 ppm; IR (KBr pellet): ṽ 3119, 3081, 2993, 2324, 2210, 1944, 1748, 1108, 1004, 945, 870, 766, 667 cm^{-1}; elemental analysis (%) for $C_3H_6N_{10}O_2$ (214.1): calcd C 16.83; H 2.82; N,65.41 Found: C 17.02; H 2.89; N 65.25.

Triaminoguanidinium [1,2,4]triazolo[4,3-b][1,2,4,5]tetrazin-3-yl(nitro)amide(9).

Silver nitrate (0.34 g, 2 mmol) was dissolved in water (5 mL) and added carefully to a solution of **3** (0.36 g, 2.0 mmol) in water (5 mL). The mixture was stirred for 2 h. After filtration, the product was obtained as a red solid **7** (0.50 g). This solid was added to the methanol solution (10 mL) of triaminoguanidinium hydrochloride (245 mg, 1.74 mmol). After stirring for 2 h at room temperature, silver chloride was removed by filtration and washed with a small amount of methanol. The filtrate was concentrated under reduced pressure and dried in vacuum to yield **9**, brown solid, 78% yield. T_d 156 °C. ^1H NMR (300 MHz, [D6]DMSO) δ 9.64 (s, 1H), 8.58 (s, 3H), 4.49 (s, 6H) ppm; ^{13}C NMR (75 MHz, [D6]DMSO) δ 159.04, 149.81, 149.73, 146.43 ppm; IR (KBr pellet): ṽ 3078, 3022, 2800, 2406, 2329, 2292, 1923, 1691, 1534, 1488, 1198, 1129, 937, 767 cm^{-1}; elemental analysis (%) for $C_4H_{10}N_{14}O_2$ (241.1): calcd C 16.79; H 3.52; N 68.51. Found: C 16.61; H 3.68; N 68.92.

1,2-bis([1,2,4]triazolo[4,3-b][1,2,4,5]tetrazin-3-yl)diazene (10).

Compound **2** (1.37 g, 10 mmol) was added to a conc. HCl (16 ml) at room temperature. After the solution becomes colorless, a solution of $KMnO_4$ (1.10 g, 6.90 mmol) in H_2O (4 ml) was added slowly (about 20 minutes) to the obtained two-phase mixture with vigorous stirring. Then the reaction mixture was stirred for a further 5 h at 50 ℃. The yellow precipitate was filter, washed with water and dried to give out a yellow compound **3** in 82% yield. T_d 305 °C; ^1H NMR (300 MHz, [D6]DMSO) δ 10.47 (s, 2H) ppm; ^{13}C NMR (75 MHz, [D6]DMSO) δ 151.74, 151.28, 149.52 ppm; IR (KBr pellet): ṽ 3102, 3030, 2852, 2788, 2543, 2438, 1519, 1420, 1345, 1265, 1201, 1138, 1074, 1013, 935, 764 cm^{-1}; elemental analysis (%) for $C_6H_2N_{14}$ (270.06): calcd C 26.67; H 0.75; N 72.58. Found: C 26.69; H 0.94; N 71.21.

6-Hydrazinyl-[1,2,4]triazolo[4,3-b][1,2,4,5]tetrazin-3-amine (12).

Hydrazine monohydrate (0.60 g, 12 mmol) was added carefully into a solution of **11** (2.31 g, 10.0 mmol) in MeCN (40 mL). The mixture was stirred for 4 h. After filtration, the product was obtained as a brown solid **12** (1.52 g), 91% yield. Td 198 °C; ^1H NMR (300 MHz, [D6]DMSO) δ 9.40 (s, 1H), 6.90 (s, 2H), 3.32 (s, 2H) ppm; ^{13}C NMR (75 MHz, [D6]DMSO) δ 157.86, 150.30, 150.13 ppm; IR (KBr pellet): ṽ 3380, 3069, 3017, 2537, 1641, 1391, 1267, 1185, 1045, 920, 740, 609 cm^{-1}; elemental analysis (%) for $C_3H_5N_9$ (167.1): calcd C 21.56, H 3.02, N 75.43. Found: C 21.51, H 3.52, N 74.87.

Tetrazolo[1,5-b][1,2,4]triazolo[3,4-f][1,2,4,5]tetrazin-8-amine (13).

To a 100-mL-jacketed beaker containing 14.4 mL of 3 M HCl was added 0.6 g (3.6 mmol) of **12**, and the suspension was stirred until complete dissolution occurred. The temperature was adjusted to -5 °C, while a solution of $NaNO_2$ (0.26 g, 3.95 mmol) in 3.6 mL of water was added dropwise and vigorous stirred for a further 1h at 0 °C. Then the solution was overnight at room temperature. The yellow precipitate was filter, washed with water and dried to give out a red compound **13** in 68% yield. Td 165 °C; ^1H NMR (300 MHz, [D6]DMSO) δ 7.64 (s, 2H) ppm; ^{13}C NMR (75 MHz, [D6]DMSO) δ 154.62, 150.61, 150.12 ppm; IR (KBr pellet): ṽ 3081, 3020, 2974, 2210, 2150, 1071, 915, 780, 724, 637 cm^{-1}; elemental analysis (%) for $C_3H_2N_{10}$ (178.0): calcd C, 20.23; H, 1.13; N, 78.6. Found: C 20.35; H, 1.26; N, 77.34.

N-(6-azido-[1,2,4]triazolo[4,3-b][1,2,4,5]tetrazin-3-yl)nitramide (14).

Compound **13** (0.71 g, 4.0 mmol) was added in portions to a mixture of HNO_3 (100%; 14.0 mL) with stirring and cooling at 0 °C. The mixture was stirred for 4 h at room temperature and afterward the solvent was removed by blowing air. Then CF_3COOH (8 mL) was added to the flask. The precipitate formed was collected by filtration and washed with CF_3COOH to give **14** (0.60 g, 67%) as an orange solid. Td 150 °C; ^1H NMR (300 MHz, [D6]DMSO) δ 9.61 (s, 1H) ppm; ^{13}C NMR (75 MHz, [D6]DMSO) δ 154.09, 146.24, 145.55 ppm; IR (KBr pellet): ṽ 3126, 3059, 2961, 2292, 2226, 2166, 1585, 1536, 1480, 1239, 1105, 939, 783, 636 cm^{-1}; elemental analysis (%) for $C_3H_2N_{10}$ (223.0): calcd C, 16.15; H, 0.45; N, 69.06. Found: C, 16.10; H, 0.57; N, 68.24.

Ammonium (6-azido-[1,2,4]triazolo[4,3-b][1,2,4,5]tetrazin-3-yl)(nitro)amide (15).

To a solution of **1** (223 mg, 1 mmol) in ethanol (5 mL) was added 25% aqueous ammonia (1.2mmol, 168 mg). The reaction was stirred at room temperature for 2h and then the solvent was evaporated in vacuo to obtain the desired product **15**, red solid, 89% yield. Td 180 °C; ^{1}H NMR (300 MHz, [D6]DMSO) δ7.09 (s, 4H) ppm; ^{13}C NMR (75 MHz, [D6]DMSO) δ 153.86, 149.72, 149.04 ppm; IR (KBr pellet): ῦ 3047, 2986, 2318, 2158, 1507, 1124, 1019, 952, 872, 706, 657 cm^{-1}; elemental analysis (%) for $C_3H_4N_{12}O_2$ (240.1): calcd C 15.00; H 1.68; N 69.99. Found: C 15.16; H 1.84; N 68.88.

Guanidinium (6-azido-[1,2,4]triazolo[4,3-b][1,2,4,5]tetrazin-3-yl)(nitro)amide (16).

To a solution of **14** (223 mg, 1 mmol) in ethanol (5 mL) was added guanidinium carbonate (0.21 g, 1.0 mmol). The reaction was stirred at room temperature for 2h and then the solvent was evaporated in vacuo to obtain the desired product **16**, red solid, 93% yield. Td 170 °C; ^{1}H NMR (300 MHz, [D6]DMSO) δ6.90 (s, 6H) ppm; ^{13}C NMR (75 MHz, [D6]DMSO) δ 157.89, 153.89, 149.62, 149.03 ppm; IR (KBr pellet): ῦ 3123, 3084, 3014, 2956, 2776, 2418, 2267, 2164, 1639, 1389, 1016, 942, 853, 767, 606 cm^{-1}; elemental analysis (%) for $C_4H_6N_{14}O_2$ (282.1): calcd C 16.96; H 2.49; N 69.24. Found: C 17.22; H 2.28; N 68.98.

Hydroxylammonium (6-azido-[1,2,4]triazolo[4,3-b][1,2,4,5]tetrazin-3-yl)(nitro) amide (17).

Silver nitrate (0.34 g, 2 mmol) was dissolved in water (5 mL) and added carefully to a solution of **14** (0.45 g, 2.0 mmol) in water (5 mL). The mixture was stirred for 2 h. After filtration, the product was obtained as a red solid (0.58 g). This solid was added to the methanol solution (10 mL) of hydroxylamine hydrochloride (123 mg, 1.76 mmol). After stirring for 2 h at room temperature, silver chloride was removed by filtration and washed with a small amount of methanol. The filtrate was concentrated under reduced pressure and dried in vacuum to yield **17**, red solid, 72% yield. Td 156 °C; ^{1}H NMR (300 MHz, [D6]DMSO) δ10.09 (s, 3H), 9.89 (s, 1H) ppm; ^{13}C NMR (75 MHz, [D6]DMSO) δ 153.87, 149.63, 148.99 ppm; IR (KBr pellet): ῦ 3172, 3128, 3100, 2727, 2626, 2263, 2159, 1489, 1432, 1331, 1033, 947, 852, 593 cm^{-1}; elemental analysis (%) for $C_3H_4N_{12}O_3$ (256.1): calcd C 14.07; H 1.57; N 65.62 . Found: C 14.07; H 1.64; N 65.51.

Triaminoguanidinium (6-azido-[1,2,4]triazolo[4,3-b][1,2,4,5]tetrazin-3-yl) (nitro)amide (18).

Silver nitrate (0.34 g, 2 mmol) was dissolved in water (5 mL) and added carefully to a solution of **14** (0.45 g, 2.0 mmol) in water (5 mL). The mixture was stirred for 2 h. After filtration, the product was obtained as a red solid (0.58 g). This solid was added to the methanol solution (10 mL) of triaminoguanidinium hydrochloride (248 mg, 1.76 mmol). After stirring for 2 h at room temperature, silver chloride was removed by filtration and washed with a small amount of methanol. The filtrate was concentrated under reduced pressure and dried in vacuum to yield **18**, brown solid, 77% yield. Td 129 °C; ^{1}H NMR (300 MHz, [D6]DMSO) δ 8.58 (s, 3H), 4.49 (s, 6H) ppm; ^{13}C NMR (75 MHz, [D6]DMSO) δ 159.02, 153.84, 149.70, 149.02 ppm; IR (KBr pellet): ῦ 3080, 3023, 3002, 2647, 2299, 2246, 2157, 1696, 1321, 1134, 1007, 867, 758, 646 cm-1; elemental analysis (%) for $C_4H_9N_{17}O_2$ (327.1): calcd C 14.68; H 2.77; N 72.77. Found: C 14.19; H 3.13; N 71.23.

1,2-bis(6-azido-[1,2,4]triazolo[4,3-b][1,2,4,5]tetrazin-3-yl)diazene (19).

Compound **5** (1.78 g, 10 mmol) was added to a Conc. HCl (16 ml) at room temperature. After the solution becomes colorless, A solution of $KMnO_4$ (1.10 g, 6.90 mmol) in H_2O (4 ml) was added slowly (about 20 minutes) to the obtained two-phase mixture with vigorous stirring. Then the reaction mixture was stirred for a further 5 h at 50 °C. The yellow precipitate was filter, washed with water and dried to give out a yellow compound **6** in 80% yield. Td 183 ℃. ^{13}C NMR (75 MHz, [D6]DMSO) δ 157.39, 150.98, 150.94 ppm; IR (KBr pellet): ῦ 3233, 3084, 3008, 2292, 2196, 2145, 1530, 1238, 1153, 1046, 970, 862, 753 cm^{-1}; elemental analysis (%) for C_6N_{20} (352.1): calcd C 20.46; H 0; N 79.54. Found: C 20.29; H 0.30; N 77.74.

Conflicts of interest

There are no conflicts to declare.

Acknowledgements

This work was supported by the Office of Naval Research (N00014-16-1-2089), the Defense Threat Reduction Agency (HDTRA 1-15-1-0028), Science and Technology Department of Sichuan Province (No. 2016JY0246), Education Department of Sichuan Province (No. 16ZB0247) and Opening Project of Sichuan Province Key Laboratory of Natural Products and Small Molecule Synthesis (No. TRCWYXFZCH2016005). We are also grateful to the M. J. Murdock Charitable Trust, Reference No.: 2014120: MNL:11/20/2014 for funds supporting the purchase of a 500 MHz NMR spectrometer.

Notes and references

1 (a) A. K. Sikder and N. A. Sikder, *J. Hazard. Mater.,* **2004**, *A112*, 1-15; (b) M. H. V. Huynh, M. A. Hiskey, D. E. Chavez, D. L. Naud and R. D. Gilardi, *J. Am. Chem. Soc.,* **2005**, 127, 12537−12543; (c) D. E. Chavez, M. A. Hiskey, D. L. Naud and D. Parrish, *Angew. Chem., Int. Ed.,* **2008**, 47, 8307−8309; (d) H. Gao and J. M. Shreeve, *Chem. Rev.,* **2011**, 111, 7377-7436; (e) X. X. Zhao, S. H. Li, Y. Wang, Y. C. Li, F. Q. Zhao, and S. P. Pang, *J. Mater. Chem. A,* **2016**, 4, 5495−5504.

2 J. P. Agrawal, Hodgson, R. D. Organic chemistry of explosive; Wiley: New York, **2007**.

3 (a) M. H. V. Huynh, M. D. Coburn, T. J. Meyer and M. Wetzler, *Proc. Natl. Acad. Sci. USA* **2006**, 103, 10322–10327; (b) K. B. Landenberger, O. Bolton and A. J. Matzger, *Angew. Chem. Int. Ed.,* **2013**, 52, 6468–6471; (c) S. Li, Y. Wang, C. Qi, X. Zhao, J. Zhang, S. Zhang and S. Pang, *Angew. Chem. Int. Ed.,* **2013**, 52, 14031-14035.

4 (a) A. M. Churakov, S. L. Ioffe and V. A. Tartakovsky, *Mendeleev Commun.,* **1995**, 6, 227-228; (b) V. Thottempudi, P. Yin, J. Zhang, D. A. Parrish and J. M. Shreeve, *Chem.-Eur. J.*, **2014**, 20, 542-548; (c) P. Yin, J. Zhang, D. A. Parrish and J. M. Shreeve, *J. Mater. Chem. A,* **2015**, 3, 8606-8612; (d) P. Yin, C. He and J. M. Shreeve, *J. Mater. Chem. A,* **2016**, 4**,** 1514-1519; (e) Y. Tang, C. He, G. Imler, D. A. Parrish and J. M. Shreeve, *Chem. Commun.,* **2018**, *54*, 10566-10569; (f) C. He, H. Gao, G. Imler, D. A. Parrish and J. M. Shreeve, *J. Mater. Chem. A*, **2018**, 6, 9391-9396.

5 (a) M. C. Schulze, B. L. Scott and D. E. Chavez. *J. Mater. Chem. A,* **2015**, 3, 17963–17965； (b) J. Zhang, P. Yin, L. A. Mitchell, D. A.

Parrish and J. M. Shreeve, *J. Mater. Chem. A,* **2016**, *4*, 7430–7436; (c) C. Bian, X. Dong, X. Zhang, Z. Zhou, M. Zhang and C. Li, *J. Mater. Chem. A,* **2015**, 3, 3594–3601; (d) D. E. Chavez, D. A. Parrish, L. Mitchell and G. H. Imler, *Angew. Chem. Int. Ed.,* **2017**, 56, 3575–3578.

6 (a) T. M. Klapötke, P. C. Schmid, S. Schnell and J. Stierstorfer, *Chem. -Eur. J.,* **2015**, 21, 9219–9228; (b) M. S. Klenov, A. A. Guskov, O. V. Anikin, A. M. Churakov, Y. A. Strelenko, I. V. Fedyanin, K. A. Lyssenko and V. A. Tartakovsky, *Angew. Chem. Int. Ed.,* **2016**, 55, 11472–11475; (c) D. G. Piercey, D. E. Chavez, B. L. Scott, G. H. Imler and D. A. Parrish, *Angew. Chem. Int. Ed.,* **2016**, 55, 15315–15318; (d) P. Yin, J. Zhang, G. Imler, D. A. Parrish and J. M. Shreeve, *Angew. Chem. Int. Ed.,* **2017**, 56, 8834–8838.

7 (a) T. M. Klapötke, Chemistry of high-energy materials, Walter de Gruyter, Berlin, **2011**, pp. 179–184; (b) P. Yin, Q. Zhang and J. M. Shreeve, *Acc. Chem. Res.,* **2016**, 49, 4–16.

8 (a) A. J. Bellamy, S. J. Ward, *Propellants, Explos., Pyrotech.,* **2002**, 27, 49–58; (b) P. Yin, L. A. Mitchell, D. A. Parrish and J. M. Shreeve, *Chem.–Asian J.,* **2017**, 12, 378–384; (c) R. D. Schmidt, G. S. Lee, P. F. Pagoria, A. R. Mitchell, *J. Heterocycl. Chem.,* **2001**, 38, 1227–1230; (d) X. Zhao, C. Qi, L. Zhang, Y. Wang, S. Li, F. Zhao and S. Pang, *Molecules*, **2014**, 19, 896–910; (e) T. D. Tran, P. F. Pagoria, D. M. Hoffman, J. L. Cutting, R. S. Lee and R. L. Simpson, 33rd International Annual Conference on ICT on Energetic Materials-Synthesis, Production and Application, Karlsruhe, Germany, **2002** June 25–28; (f) W. Xu, C. An, J. Wang, J. Dong and X. Geng, *Propellants, Explos., Pyrotech.,* **2013**, 38, 136–141; (g) Y. Wang, Y. Liu, S. Song, Z. Yang, X. Qi, K. Wang, Y. Liu, Q. Zhang and Y. Tian, *Nat. Commun.,* **2018**, 9 , 1–11.

9 (a) D. Izsák, T. M. Klapötke, F. H. Lutter and C. Pflüger, *Eur. J. Inorg. Chem.,* **2016**, 2016, 1720-1729; (b) Y. Tang, C. He, L. A. Mitchell, D. A. Parrish and J. M. Shreeve, *J. Mater. Chem. A*, **2015**, 3, 23143-23148.

10 (a) J. Ma, G. Cheng, X. Ju, Z. Yi, S. Zhu, Z. Zhang and H. Yang, *Dalton Trans.,* **2018**, 47, 14483-14490; (b) L. Hu, P. Yin, G. Zhao, C. He, G. H. Imler, D. A. Parrish, H. Gao and J. M. Shreeve, *J. Am. Chem. Soc.*, **2018**, 140 , 15001-15007.

11 (a) C. He and J. M. Shreeve, *Angew. Chem. Int. Ed.,* **2016**, 55, 772 – 775; (b) T. M. Klapötke, D. G. Piercey, N. Mehta, K. D. Oyler, M. Jorgensen, S. Lenahan, J. S. Salan, J. W. Fronabarger and M. D. Williams, *Z. Anorg. Allg. Chem.,* **2013**, 639, 681 –688.

12 (a) J. W. Fronabarger, M. D. Williams, W. B. Sanborn, J. G. Bragg, D. A. Parrish, M. Bichayc, *Propellants Explos. Pyrotech.,* **2011**, 36, 541–550; (b) D. Fischer, T. M. Klapötke and J. Stierstorfer, *Angew. Chem. Int. Ed.,* **2015**, 54, 10299–10302; (c) T. M. Klapötke and N. Mehta, *Propellants Explos. Pyrotech.,* **2014**, 39, 7–8; (d) Q. Yu, G. H. Imler, D. A. Parrish and J. M. Shreeve, *Dalton Trans.,* **2018**, 47, 12661-12666.

13 (a) T. Brinck, Green Energetic Materials, Wiley, Hoboken, **2014**; (b) T. Musil, R. Matyáš, R. Vala, A. Růžička and M. Vlček, *Propellants, Explos., Pyrotech.,* **2014**, 39, 251–259; (c) D. D. Ford, S. Lenahan, M. Jörgensen, P. Dubé, M. Delude, P. E. Concannon, S. R. Anderson, K. D. Oyler, G. Cheng, N. Mehta, J. S. Salan, *Org. Process Res. Dev.,* **2015**, 19, 673–680.

14 D. Chen, H. Yang, Z. Yi, H. Xiong, L. Zhang, S. Zhu and G. Cheng, *Angew. Chem. Int. Ed.,* **2018**, 57, 2081–2084.

15 J. P. Agrawal, High energy materials: propellants, explosives and pyrotechnics, T. J. International Ltd, Great Britain, **2010**.

16 (a) R. A. Carboni and J. E. Castle, *J. Am. Chem. Soc.,* **1962**, 84, 2453-2454; (b) T. Urbanski, Chemistry and Technology of Explosives, Pergamon, Oxford, **1984**, vol. 4, p. 206; (c) T. M. Klapötke and T. Witkowski, *ChemPlusChem*., **2016**, 81, 357-360; (d) X. Zhang, H. Xiong, H. Yang and G. Cheng, *New J. Chem.,* **2017**, 41, 5764-5769.

17 C. Li, M. Zhang, Q. Chen, Y. Li, H. Gao, W. Fu and Z. Zhou, *Dalton Trans.,* **2016**, 45, 17956-17965.

18 P. Yin, L. A. Mitchell, D. A. Parrish and J. M. Shreeve, *Angew. Chem. Int. Ed.,* **2016**, 55, 14409 –14411.

19 J. Zhang, Q. Zhang, T. T. Vo, D. A. Parrish and J. M. Shreeve, *J. Am. Chem. Soc.,* **2015**, 137, 1697−1704.

20 G. F. Rudakov, Y. A. Moiseenko and N. A. Spesivtseva, *Chem. Heterocycl. Compd.,* **2017**, 53, 802-810.

21 D. E. Chavez and M. A. Hiskey, *J. Heterocycl. Chem.,* **1998**, 35, 1329-1332.

22 T. M. Klapötke and D. G. Piercey, *Inorg. Chem.,* **2011**, 50, 2732–2734.

23 D. E. Chavez, M. A. Hiskey and R. D. Gilardi, *Angew. Chem. Int. Ed.*, **2000**, *39*, 1791-1793.

24 M. J. Frisch, G. W. Trucks, H. B. Schlegel, G. E. Scuseria, M. A. Robb, J. R. Cheeseman, J. A. Jr. Montgomery, T. Vreven, K. N. Kudin, J. C. Burant, J. M. Millam, S. S. Iyengar, J. Tomasi, V. Barone, B. Mennucci, M. Cossi, G. Scalmani, N. Rega, G. A. Petersson, H. Nakatsuji, M. Hada, M. Ehara, K. Toyota, R. Fukuda, J. Hasegawa, M. Ishida, T. Nakajima, Y. Honda, O. Kitao, H. Nakai, M. Klene, X. Li, J. E. Knox, H. P. Hratchian, J. B. Cross, V. Bakken, C. Adamo, J. Jaramillo, R. Gomperts, R. E. Stratmann, O. Yazyev, A. J. Austin, R. Cammi, C. Pomelli, J. W. Ochterski, P. Y. Ayala, K. Morokuma, G. A. Voth, P. Salvador, J. J. Dannenberg, V. G. Zakrzewski, S. Dapprich, A. D. Daniels, M. C. Strain, O. Farkas, D. K. Malick, A. D. Rabuck, K. Raghavachari, J. B. Foresman, J. V. Ortiz, Q. Cui, A. G. Baboul, S. Cli fford, J. Cioslowski, B. B.; Liu, G.; Liashenko, A.; Piskorz, P.; Komaromi, I.; Martin, R. L.; Fox, D. J. Stefanov, T. Keith, M. A. Al-Laham, C. Y. Peng, A. Nanayakkara, M. Challacombe, P. M. W. Gill, B. Johnson, W. Chen, M. W. Wong, C. Gonzalez, J. A. Pople, Gaussian 03, revision D.01; Gaussian, Inc.: Wallingford, CT, **2004**.

25 A. A. Dippold and T. M. Klapötke, *Chem. Asian J.* **2013**, 8, 1463 – 1471.

26 M. Sucéska, EXPLO5, *Version 6.01*, Brodarski Institute, Zagreb, Croatia, **2013**.

27 (a) U. M. Regulations, *UN Recommendations on the Transport of Dangerous Goods, Manual of Tests and Criteria*, 5th edn, United Nations Publication, New York, **2009**; (b) 13.4.2 Test 3 (a)(ii) BAM Fallhammer, p. 75; c) 13.5.1 Test 3 (b)(i): BAM friction apparatus, p. 104.

28 S. K. Wolff, D. J. Grimwood, J. J. McKinnon, M. J. Turner, D. Jayatilaka, M. A. Spackman, CrystalExplorer, version 3.1; University of Western Australia: Crawley, Australia, **2012**.

29 J. Zhang, J. Zhang, D. A. Parrish and J. M. Shreeve, *J. Mater. Chem. A,* **2018**, 6, 22705-22712.

30 M. S. Westwell, M. S. Searle, D. J. Wales and D. H. Williams, *J. Am. Chem. Soc.*, **1995**, 117, 5013-5015.

31 H. Gao, C. Ye, C. M. Piekarski and J. M. Shreeve, *J. Phys. Chem. C*, **2007**, 111, 10718-10731.

32. Bruker (2015). *APEX3 v2015.5-2*. Bruker AXS Inc., Madison, Wisconsin, USA, 2015.

33. Bruker (2013). *SAINT v8.34A*. Bruker AXS Inc., Madison, Wisconsin, USA, 2013.

34. Bruker (2014). *XPREP v2014/2*. Bruker AXS Inc., Madison, Wisconsin, USA, 2014.

35. Bruker (2014). *SADABS v2014/5*, Bruker AXS Inc., Madison, Wisconsin, USA, 2014.

36. Sheldrick, G. M. *(2014). SHELXL-2014/7*. University of Göttingen, Germany., 2014

TOC

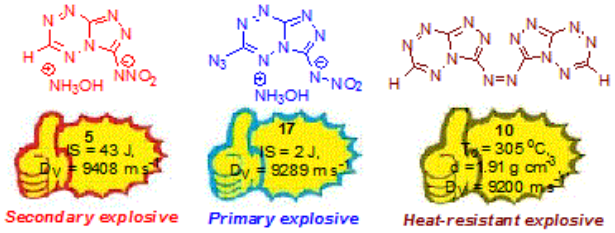

Next-generation fused ring energetic materials for different applications were designed by regulating mechanical sensitivity.